THE MECHANISM OF STRESS INFLUENCE ON SWELLING OF 20% COLD WORKED 16Cr15Ni2MoTiMnSi STEEL—I. A. Portnykh, A. V. Kozlov, V. L. Panchenko (FSUE Institute of Nuclear Materials), V. M. Chernov (A. A. Bochvar Institute of Inorganic Materials), and F. A. Garner (Pacific Northwest National Laboratory)

OBJECTIVE

The object of this effort is to explore new mechanisms whereby environmental variables such as applied stress can affect radiation-induced microstructural evolution of structural alloys of fusion devices. New insight on these mechanisms will lead to better predictions in fusion environments.

SUMMARY

Argon-pressurized tubes of 20% cold-worked 16Cr15Ni2MoTiMnSi steel were irradiated at hoop stresses of 0, 100, and 200 MPa at ~740K in the BN-600 fast reactor to 108 dpa. Following nondestructive measurements of strain, density measurements and microscopy were conducted. Voids were categorized into three types depending on their association with other microstructural features. Stress enhanced the nucleation of all void types, but nucleation of voids associated with dislocations was increased the most. Swelling increased as a consequence, even though the average size of each type void decreases. Swelling measured by TEM and density change gave identical results.

A stress-enhanced void nucleation model is presented to explain these results. It invokes collection and diffusion of helium-vacancy complexes in dislocation cores and intersections to produce void nuclei, followed by stress-induced breakaway of the pinned dislocation to reach new obstacles and initiate the next sequence of helium collection and void nucleation.

PROGRESS AND STATUS

Introduction

Applied mechanical stress is one of the important variables that are known to accelerate the onset of void swelling [1]. Most studies show that stress results in a significant increase of swelling [2] while a few other studies show a very small or no effect [3]. At present, there is no quantitative model for confident prediction of the influence of stress on swelling. Additional data are required to develop a predictive model. Toward this objective, this paper examines the effect of a biaxial stress state on the swelling of 20% CW 16Cr15Ni2MoTiMnSi austenitic steel at very high neutron exposure.

Experimental Procedure

Three argon-pressurized tubes of 70 mm length, 6.9 diameter, and 0.4 mm wall thickness were fabricated from 20% cold-worked steel of composition Fe-15.45Cr-14.80Ni-2.37Mo-1.29Mn-0.44Si-0.06C-0.014P-0.004S in wt %. Internal pressures of 0, 52, and 104 atm were used to produce hoop stresses of 0, 100, and 200 MPa during side-by-side irradiation in flowing sodium at ~740K in the BN-600 fast reactor to 108 dpa at 1.9×10^{-6} dpa/sec [4]. The outer diameters were measured before and after irradiation by a profilometry technique. Measurements were made at 12 axial locations and 5 radial positions and the measurements were averaged. After irradiation, the tubes were destructively examined. After removing the end caps, the density change of the tube was determined via hydrostatic weighing. Electron microscopy was used to study the microstructure. The quantitative method employed for microscopy analysis was presented previously [5, 6].

Results

Table 1 and Fig. 1 present the diameter and density change measurements as well as the microscopy determinations of swelling. While swelling increases almost linearly with stress, the creep deformation may exhibit some small nonlinearity but could be approximated by a linear relationship. With only three data points, these two possibilities can not be distinguished. The creep deformation CD was

calculated as $CD = \frac{\Delta d}{d} - \frac{1}{3} \cdot S$, where S = S_d, the swelling determined by density change. The swelling determined by microscopy is subjected to greater measurement errors and scatter, but appear to be in agreement with the bulk-averaged density change results.

TEM examination of multiple areas of each specimen showed that different porosity distributions developed as a function of stress. Figure 2 shows typical void micrographs at each stress level.

Voids were identified in four categories as described elsewhere [5, 6]: *a*-type voids are arrayed on dislocations, *b*-type voids are associated with precipitates, usually involving two separate distributions, and free-standing *c*-type voids formed on gas-vacancy complexes in the crystal matrix.

Table 1. Results of diameter and density measurements

Cladding stress, MPa	Mean value of diameter, mm	Diameter change $\Delta d/d_0$, %	Density, g/cm^3	Swelling %, Density S_d	Swelling %, TEM S_{TEM}	Creep deformation, CD %
Unirradiated specimen	6.92	-	7.94	-	-	-
0	7.12	2.89	7.30	8.8	8.6	0.0
100	7.30	5.49	7.17	10.7	10.5	1.9
200	7.57	9.39	7.07	12.3	12.5	5.3

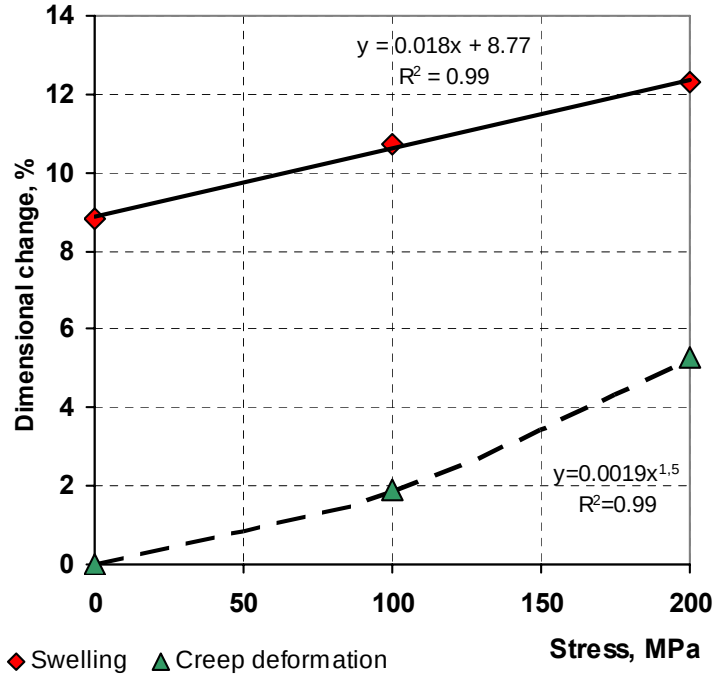

Fig. 1. Swelling and creep deformation as a function of stress.

Electron-microscopy examinations revealed different porosity characteristics for specimens irradiated without stress and under stress. Fig. 2 presents typical micrographs. In general, homogeneous distributions of voids were observed in specimens irradiated at 0 and 200 MPa, with somewhat more heterogeneity observed at 100 MPa. The largest volume fraction of voids in the specimens without stress was the b-type voids connected with G-phase precipitates, while the largest voids were usually located on twins.

Histograms of the void-size distribution are shown in Fig. 3 with single distributions obtained by the χ^2 criterion [4], described as the sum of the four single distributions as follows: *a*-type voids are formed on dislocations, *b*-type voids of two types connected with precipitates, and *c*-type voids formed on gas-vacancy complexes in the crystal matrix, the latter having smallest sizes [5]. A summary of mean sizes and concentrations of each void type is shown in Fig. 4. Note that the contribution of b-type voids to total swelling decreases with increasing stress as shown in Fig. 5. The enhancement of void swelling by stress is reflected in a pronounced increase in void density, especially in the density of *a*-type voids, but the increase is not reflected in the void sizes, which uniformly decrease with stress.

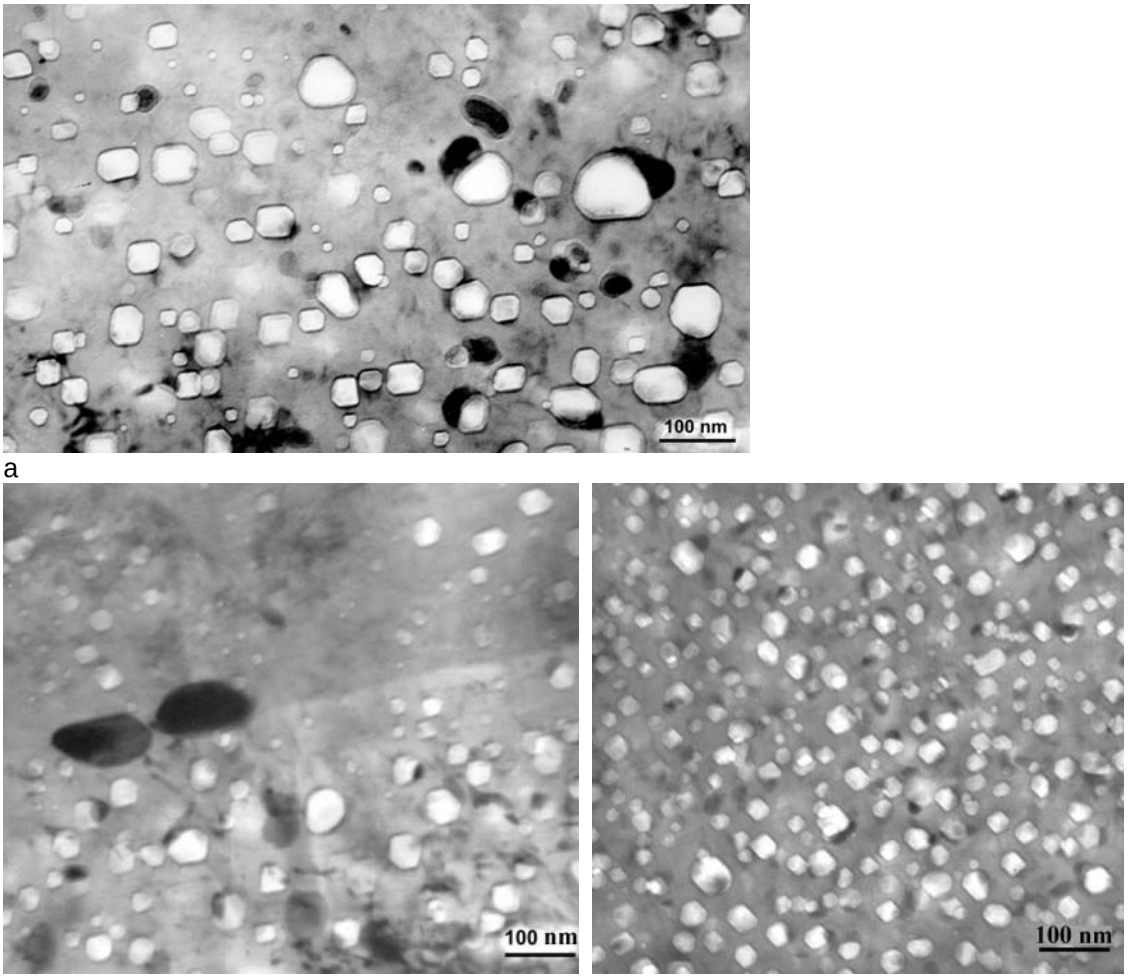

Fig. 2. Voids and precipitate microstructures observed at a) 0, b) 100, and c) 200 MPa. Most of the precipitates are G-phase.

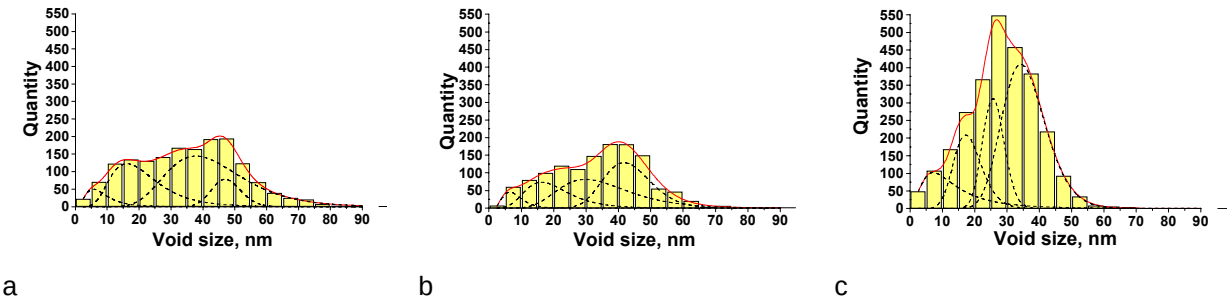

Fig. 3. Void-size distributions at a) 0 MPa, b) 100 MPa, and c) 200 MPa. The total number of voids measured was 1600, 1300, and 2700, respectively. ▭ - experimental data, – – - single log-normal distribution, ▬ - sum of single log-normal distributions.

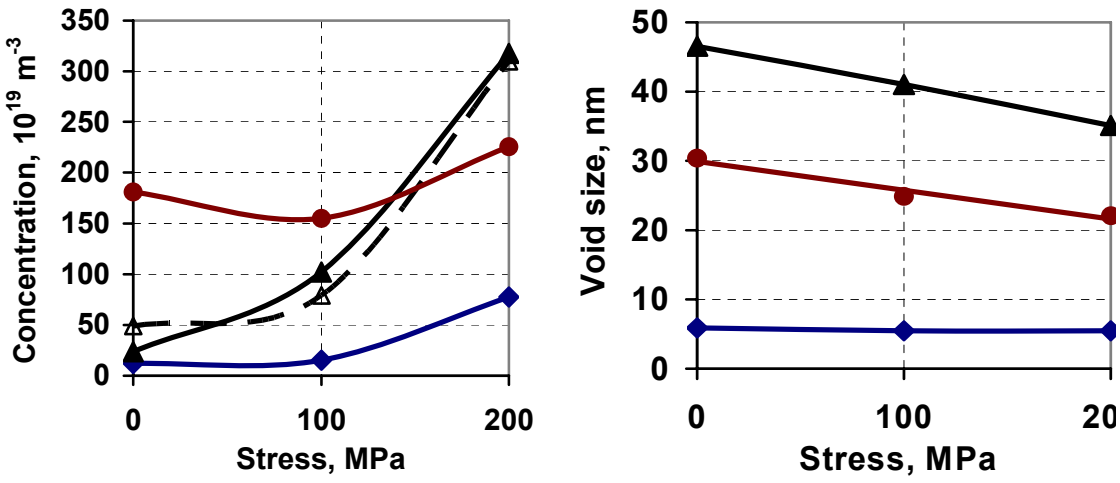

a b

Fig. 4. Dependence of concentration (a) and mean size (b) on stress for each type of voids: ▲ - *a*-type, ● - *b*-type, and ◆ - *c*-type, △ - theoretical prediction of *a*-type based on our model.

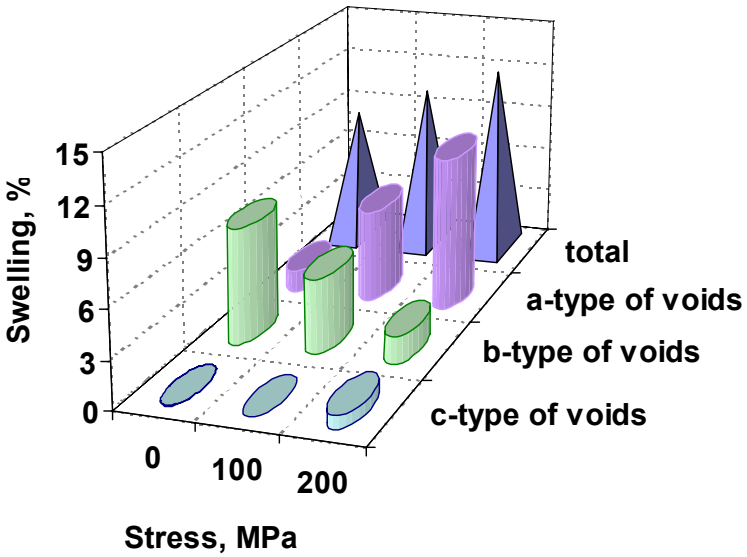

Fig. 5. Contribution to total swelling of each type of void.

Discussion

It can be shown that stress at ~200 MPa cannot significantly influence the diffusion characteristics of point defects and therefore, cannot significantly change the growth rate of voids, but stress can strongly influence void nucleation, as demonstrated in this experiment. It appears that void nucleation of the a-type voids is particularly sensitive to the stress level. We advance here a new explanation to explain this result. This model assumes that stabilization of void nuclei requires helium and stress can alter the way in which helium is collected and bubbles distributed.

Transmutant helium (with concentration determined as 1 appm/dpa for the BN-600 reactor [7]), when combined with a vacancy, migrates as a gas-vacancy pair, with mobility determined by the vacancy migration energy of ~1.2–1.3 eV [7]. In the dislocation core, this pair diffuses with migration energy of ~0.6 eV. This pipe diffusion causes He-vacancy bubbles to be formed on dislocations, especially where dislocations intersect, producing void nuclei after reaching a critical size. This mechanism was proposed earlier to explain *a*-type void growth, especially in the early stages of swelling at 650–800K [8].

When the local stress exceeds a critical value σ_c, the dislocation slips over any obstacles that pin it and then glides to the next group of obstacles. Voids or bubbles earlier formed on a dislocation stay in their original position and continue to grow. The dislocation in its new location begins to collect He-vacancy pairs and generate new nuclei. This process is repeated each time the dislocation moves, leading to stress enhancement of voids.

If an external stress σ is applied to a dislocation and requires an additional stress $(\sigma_c - \sigma)$ by accumulation of point defects to overcome the obstacles, then τ is mean time required to achieve dislocation separation and is proportional to the additional stress. The number of voids forming per time *t* can be expressed as follows:

$$n_a = n_{a_0} + \xi_n \cdot \rho_d \cdot \frac{t}{\tau} = n_{a_0} + \frac{\xi_n \cdot \rho_d \cdot \nu_\sigma \cdot t}{(\sigma_c - \sigma)} = n_{a_0} + \frac{A}{(\sigma_c - \sigma)} \qquad (1)$$

where

ξ_n – number of voids per length unit, formed on dislocation during its immovable state,
ρ_d – dislocation density,
ν_σ – coefficient characterizing the rate of internal stress accumulation due to defect accumulation, and
n_{a_0} – concentration of voids, formed on a stationary dislocation in absence of applied stress.

Figure 4a contains a theoretical prediction of a-type behavior using this model, where *A* and σ_c were determined by optimization to fit the experimental data. One can see a qualitative coincidence between experimental and calculated curves illustrating some success of the proposed model to describe stress-induced swelling. The dependence of mean size of *a*-type voids on stress exhibited in Fig. 4b is additional indirect confirmation of this model.

Conclusions

Void swelling of pressurized tubes constructed from 20% cold-worked 16Cr15Ni2MoTiMnSi austenitic steel and irradiated at 740 K to 108 dpa in the BN-600 fast reactor clearly show that applied stress enhances swelling. The enhancement is manifested primarily as a strong increase in the void density, especially those voids which are associated with dislocations. A new model is presented to explain these results that involve collection and diffusion of helium in dislocation cores, followed by stress-induced breakaway from pinning points, leading to a new sequence of collection and nucleation.

Acknowledgements

This work was supported by a grant of the Russian Federation President for State Support of Young Scientists, No. MK-20011.2005.2. F. A. Garner's participation was funded by the U.S. Department of Energy, Office of Fusion Energy.

References

[1] F. A. Garner, Chapter 6: Vol. 10A of Materials Science and Technology: A Comprehensive Treatment, VCH Publishers (1994) 419.
[2] H. R. Brager, F. A. Garner, and G. L. Guthrie, J. Nucl. Mater. 66 (1977) 301.

[3] K. Herschbach, W. Schneider, and H.-J. Bergman, Effects of Radiation on Materials: 14th International Symposium (Vol. II), ASTM STP 1046 (1990) 570.
[4] S. A. Averin, A. V. Kozlov, N. I. Budylkin, and V. V. Romaneev, Investigations of Structural Materials of Fast Sodium Reactor Core, collected articles, RAS UD, Ekaterinburg (1994) 153, in Russian.
[5] I. A. Portnykh and A. V. Kozlov, VANT quarterly report series: Material science and new materials, No.1 (59) (2002) 41, in Russian.
[6] I. A. Portnykh, A. V. Kozlov, and L. A. Skryabin, Perspective Materials No. 2 (2002) 50, in Russian.
[7] A. G. Zalyzhnyi, Lu. N. Sokyrskiy, and V. N. Tebys, Energoatomizdat, Moscow (1988) 224, in Russian.
[8] I. A. Portnykh, V. Sagaradzhe, A. V. Kozlov, and L. A. Skryabin, PhMM, Vol. 94, No. 1 (2002) 105, in Russian.